Research on Engineering Structures & Materials
www.jresm.org
Research Group

Research Article

Determination of wear rate and coefficient of friction of Al6262 reinforced with different weight percentage of WC/MoS_2 under dry sliding condition

Kadapa Hemadri[1,a], Ajith Arul Daniel S[1,b], Vijayendra Kukanur[2,c], Madeva Nagaral[3,d]

[1]*Dept. of Mechanical Eng., Vels Institute of Science, Technology & Advanced Studies, Tamil Nadu India*
[2]*Dept. of Mechanical Eng., H.K.E.Society's Sir.M.Visvesvaraya College of Engineering, Karnataka India*
[3]*Aircraft Research and Design Centre, HAL, Bengaluru, Karnataka, India*

Article Info

Article history:

Received 09 Oct 2023
Accepted 31 Jan 2024

Keywords:

Tungsten carbide;
Molybdenum di Sulphide;
Wear;
Taguchi;
SEM analysis

Abstract

A tribological investigation was undertaken on hybrid metal matrix composites based on Aluminum alloy 6262, incorporating varying weight percentages of Tungsten Carbide (WC) and Molybdenum disulfide (MoS_2) under dry sliding conditions. Specifically, Tungsten Carbide was incorporated at 3%, 6%, and 9%, while Molybdenum disulphide was introduced at 2%, 4%, and 6%. The fabrication of these hybrid composites was accomplished using the stir casting technique. The experimental design followed an L27 orthogonal array, and Taguchi optimization was employed to identify the optimal combination of input parameters. The orthogonal array, signal-to-noise ratio and analysis of variance were employed to study the optimal testing parameters on developed composites. The optimal formulation, resulting in the minimum wear rate and coefficient of friction, was determined to be 9% WC, 6% MoS2, a load of 10N, a sliding velocity of 1 m/s, and a sliding distance of 400 m. Characterization was carried out for Al6262/WC/MoS_2 hybrid composite by using scanning electron microscopy (SEM).

1. Introduction

In the field of composite materials, numerous investigations have been carried out. It exhibits higher material performance in comparison to traditional materials. A common composite, particularly in the automotive and aerospace industries, is aluminum-based material. This is due to its accessibility, affordable production costs, and simplicity of manufacturing [1-4]. The devices' everyday mechanical components are susceptible to wear and tear. Wear-resistant materials should be utilized in the machine in order to boost its reliability [5]. The automotive industry is placing greater focus on weight optimization since it lowers emissions and improves fuel economy. Aluminum alloys are being used more often because they help reduce weight and have other advantages including strong corrosion resistance, good formability, and recyclability [6]. A great deal of research has been done on the wear of aluminum composites. Stir casting is the most often used production technique for producing composites among many others [6]. Furthermore, the main issue with their usages includes deteriorated performance at high temperatures and poor friction coefficient and wear rate [7]. MMCs, which are hard ceramic elements reinforced in aluminum alloys, are used to solve these issues. Due to its increased

*Corresponding author: madev.nagaral@gmail.com
[a] orcid.org/0000-0003-6892-1020; [b] orcid.org/0000-0002-7279-8491; [c] orcid.org/0000-0002-6892-1020; [d] orcid.org/0000-0002-8248-7603
DOI: http://dx.doi.org/10.17515/resm2024.09me1009rs

toughness, high stiffness, and excellent wear resistance, aluminum-based MMC is being employed more and more in these industries [8].

The addition of particles of hard ceramic is what has caused these increases in tribological properties. Wear is a major effect in the operation of many automotive components, including pistons, cylinder liners, connecting rods etc. [9]. These components are all made of aluminum-based MMC. The lowest wear rate was attained by experimenting Al/SiC nanocomposites with a 2-volume percent graphite addition the combined due to its self-lubricating properties [10]. Also, another research positive impact of soft MoS_2 particles improvements in Al/Al_2O_3 composites' wear resistance and friction. Between touching surfaces, a protecting layer is created primary factor lowering the hybrid wear composites enhanced aluminum resistance to abrasion alloys through the creation of a hybrid composites. By adopting the stir casting technique [11], Al2219 combined with B_4C & MoS_2 for composite materials. In the experiment, the morphology, density, micro hardness, tensile strength, and dry sliding wear test are all evaluated. The outcome shows that, as observed in the morphology of the matrix alloy, the reinforcement particles are spread arbitrarily and finely. In comparison to prepared composite material, Al2219 alloy has a comparatively low density and microhardness. Al2219 and MoS2 have a minimum mechanical property and Al2219 alloy has a maximum tensile strength. Wear rate is reduced, and their wear resistance is increased by the addition of MoS2 reinforcement [12]. Radhika and Jojith investigated the tribological properties of $LM13/TiO_2/MoS_2$. They take into account the applied force applied, sliding velocity, and sliding distance are their input parameters. In this work, the author used the Taguchi approach to determine sliding wear and came to the conclusion that TiO_2/MoS_2 reinforced offers superior abrasion resistance [13]. Al6061/SiC/WC hybrid aluminum materials have been attempted under various weight percentages of reinforcement particulates [13]. The addition of stiffer and stronger reinforcement to the matrix material has boosted the hardness of AMMCs. The compression, tensile, and fatigue strength of the aluminum composite material can all be greatly improved by the addition of SiC and WC reinforcements to the matrix alloy [14].

2. Experimental Setup

As a matrix material, Al 6262 has been selected because of its good material qualities, high level of resistance to corrosion, and great weldability. Because of its inherent ability to lubricate itself, MoS_2 is used as reinforcement. Table 1 below illustrates the base material's chemical make-up. Before being cast, the reinforcements is heated for 25 minutes at 450°C. After warming the reinforcement, the Al6262 was melted in a graphite crucible at 550°C to 650°C. In order to prevent explosives, magnesium is added at 2% wrapped in aluminum foil and added to the aluminum matrix. After the reinforcement added all the materials is then stirred for 10 minutes at 800 rpm [15]. While the combination of Aluminum 6262, tungsten carbide, and molybdenum disulfide (MoS_2) offers several limitations, combining these materials may pose challenges during the manufacturing process, especially in terms of fabrication, machining, or bonding. Specialized processes may be required, increasing production complexity. The Pin on Disc setup was used to find the wear rate of the developed composites. The EDAX analysis of the developed composites is shown in figure 1. The chemical combination of the base material is shown in Table 1.

Wear rate (Wi) was then calculated by calculating using the following equation :

$$W_i = \frac{V}{LnS} \tag{1}$$

where V is volume rate and n are the applied load on ring and S is the sliding distance. The coefficient of friction can be calculated as follows.

$$Ff = \mu^* N \quad (2)$$

Ff is the frictional force, μ is the coefficient of friction, and N is the applied normal load

Table 1. Typical chemical composition for aluminum alloy 6262

Si	Fe	Cu	Mn	Mg	Zn	Ti	Pb	Bi	Cr	Al
0.80	0.25	1.4	0.75	1.05	0.15	0.10	0.55	0.60	0.23	94.12

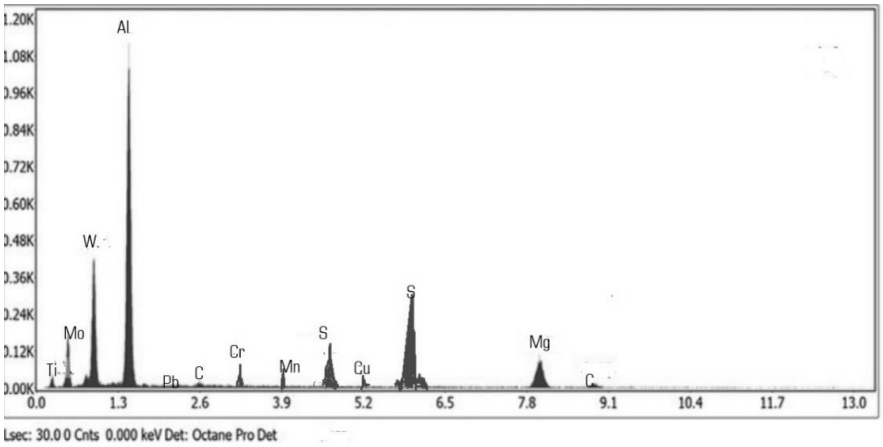

Fig. 1. EDAX analysis of the composites

3. Design of Experiments

The table 3 shows design of experiments used in this study is with five factor and three levels. The input parameters are wight percentage of tungsten carbide, weight percentage of molybdenum disulphide, load, sliding velocity and sliding distance. The Brinell hardness value of the composites is shown in table 2. When the weight percentage of the composites increases and the percentage of MoS_2 in intermediate level the hardness values is higher. When the volume fraction of the reinforcement in the composite is a critical factor. Increasing the volume fraction of reinforcement generally tends to enhance hardness up to a certain point. The uniform distribution of reinforcement particles within the Al 6262 matrix is essential. Agglomeration or uneven distribution can lead to localized variations in hardness. The output parameters are wear rate and coefficient of friction. Based upon these criteria L27 orthogonal array is chosen for performing the experiments as shown in Table 3.

Table 2. Hardness of the composites

WC	3	3	3	6	6	6	9	9	9
MoS_2	2	4	6	2	4	6	2	4	6
BHN	76	80.2	75.6	81.5	84.3	80.2	87.6	92.2	86.7

Table 3. L27 Levels and factors

Factors	Unit	Level 1	Level 2	Level 3
WC	%	3	6	9
MoS2	%	2	4	6
Load	N	10	20	30
Sliding Speed	m/sec	1	1.5	2
Sliding Distance	m	400	800	1200

4. Results and Discussion

4.1 S/N Ratio and ANOVA

The figure 2 shows the Signal to noise ratio of wear rate. The decrease in wear rate trends to lower weight percentage of tungsten carbide. The results show that at 3 % of WC offers maximum wear rate. This is due to the hardness of the composite material. It is generally believed that contribution of hard particles to aluminum alloys results in an improvement of the wear resistance of the base alloy to a great extent [16]. At 3% of tungsten carbide the hardness of the composites is less. Owing to this tendency the density of the material is less which results increase in wear rate. In addition to 6% and 9% the hardness increases and the wear rate also reduces. In addition of MoS_2 the hardness starts increasing in addition of MoS_2 percentage. When MoS2 is at 6% at WC at 9% the hardness of the material is higher. Due to increase in percentage of MoS_2 the self-lubricant properties of the materials increase which reduces the friction between the pin and the disc reduces which trends to loss of materials [17].

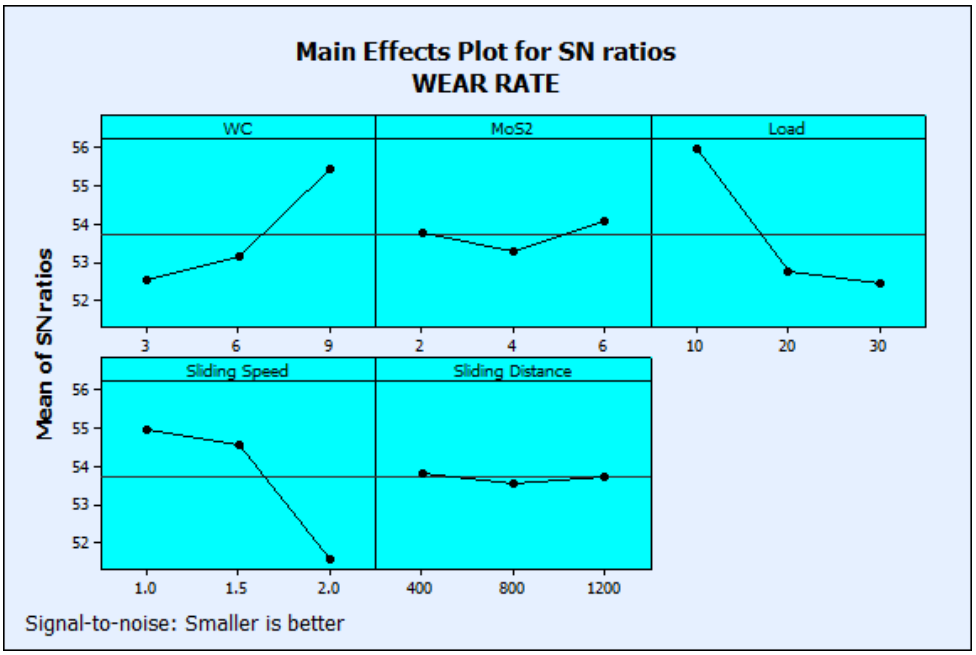

Fig. 2. S/N ratio graph for wear rate

Table 4. L27 orthogonal array and experimental results

	WC	MoS2	Load	Sliding Speed	Sliding Distance	Wear Rate	COF
1	3	2	10	1	400	0.00155	0.206
2	3	2	10	1	800	0.0015	0.236
3	3	2	10	1	1200	0.00165	0.255
4	3	4	20	1.5	400	0.002	0.308
5	3	4	20	1.5	800	0.0024	0.353
6	3	4	20	1.5	1200	0.00334	0.428
7	3	6	30	2	400	0.003	0.486
8	3	6	30	2	800	0.00345	0.453
9	3	6	30	2	1200	0.00365	0.476
10	6	2	20	2	400	0.00354	0.451
11	6	2	20	2	800	0.00342	0.472
12	6	2	20	2	1200	0.0025	0.334
13	6	4	30	1	400	0.00265	0.354
14	6	4	30	1	800	0.00205	0.297
15	6	4	30	1	1200	0.0023	0.311
16	6	6	10	1.5	400	0.00158	0.201
17	6	6	10	1.5	800	0.00155	0.189
18	6	6	10	1.5	1200	0.00131	0.177
19	9	2	30	1.5	400	0.00156	0.207
20	9	2	30	1.5	800	0.00182	0.245
21	9	2	30	1.5	1200	0.00192	0.287
22	9	4	10	2	400	0.00157	0.205
23	9	4	10	2	800	0.00193	0.216
24	9	4	10	2	1200	0.00176	0.201
25	9	6	20	1	400	0.00181	0.226
26	9	6	20	1	800	0.00165	0.248
27	9	6	20	1	1200	0.00127	0.165

The harder deformation of the counter surface penetrates the softer pin surface more as the applied stress increases. After each composite's critical load [18], with the application of load, the wear rate quickly starts to rise when the applied load increases to 20 N. The load at 30N the wear rate spikes to a very high level. In the event that the transitional load and the velocity of the composite increases in value by a large margin. Here is due to the noticeably greater frictional heating and as a result the pin material's localized adhesion to the counter surface as well as a rise in the surface structure's softening and more asperities can penetrate as a result larger deformation in wear surface are acquired [19]. The impacts graphic demonstrates that sliding speed is the parameter with the greatest relative impact. The plot clearly shows that wear rate of the composites reduces with sliding distance and reinforcement material but increases with sliding velocity [20]. It is common knowledge that the elastic modulus and temperature-related characteristics of composite materials can influence their tribological behavior. When two materials slide

against one another, heat is produced at the deformation, which raises the temperature at the interface and affects how viscoelastic the materials' reaction to tension. The temperature at the friction surface rises as sliding velocity increases, which may substantially impair the mechanical properties of the composites and cause significant loss in composite materials [21].

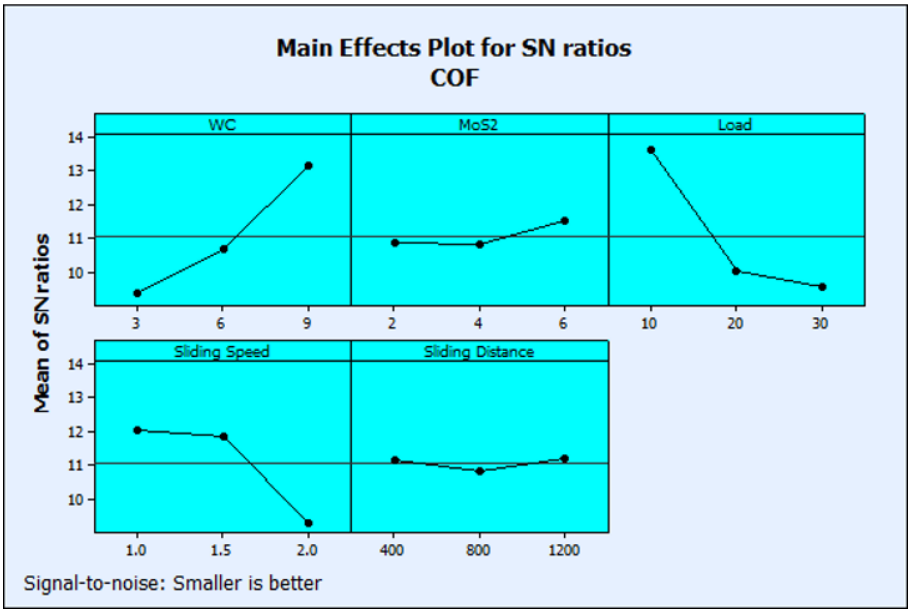

Fig. 3 S/N ratio graph for coefficient of friction

The Figure 3 shows the Signal to noise ratio of Coefficient of friction. The weight percentage of the tungsten carbide is the most significant parameters in friction coefficient. The initial finding in terms of the results is the drop in coefficient of friction as a result of an increase in the reinforcement's weight percentage. Comparing the reinforced AMMNCs to aluminum 6262 alloy indicated a lower coefficient of friction. It can be attributed to the composite's increased hardness, which results from the combination of abrasive particles and behaves as a tougher substance within the matrix [22]. Good surface adhesion occurs between the matrices and non-reinforcement whenever refractory bits are firmly bonded to the matrix. According to numerous studies, the COF of crystalline MoS_2 is typically low, at 6% in a dry sliding condition, this lubricating performance of MoS_2 is unique due to its self-lubrication properties. One explanation for this is that in a dry environment, MoS_2 particles good has adhesion and smaller particle sizes can easily fill the substrate's rough surface. Additionally, the reciprocating shear stress that occurs during the frictional process can disintegrate MoS_2 particles into lamella, resulting in a reduction in the sliding friction coefficient [23].

The COF are increased from 10N to 30N. When a force of 10N is applied, the WC percentages significantly increase the substrate's hardness of the composites and keep abrasive particles from becoming embedded in the contact area, effectively preventing cutting on friction. In the meantime, the interface's shear strength is outweighed by the cohesive force between the WC and the matrix materials. As a result, there is hardly any WC particle pull away first from contact area. As a result, compared to certain other loads, the COF at a 10N load is considerably less. When the load reaches 30N, the ultimate stress

begins to outweigh the binding effect between the WC and the substrates, leading to WC continuous extraction and cohesiveness occurs which leads higher friction coefficient.

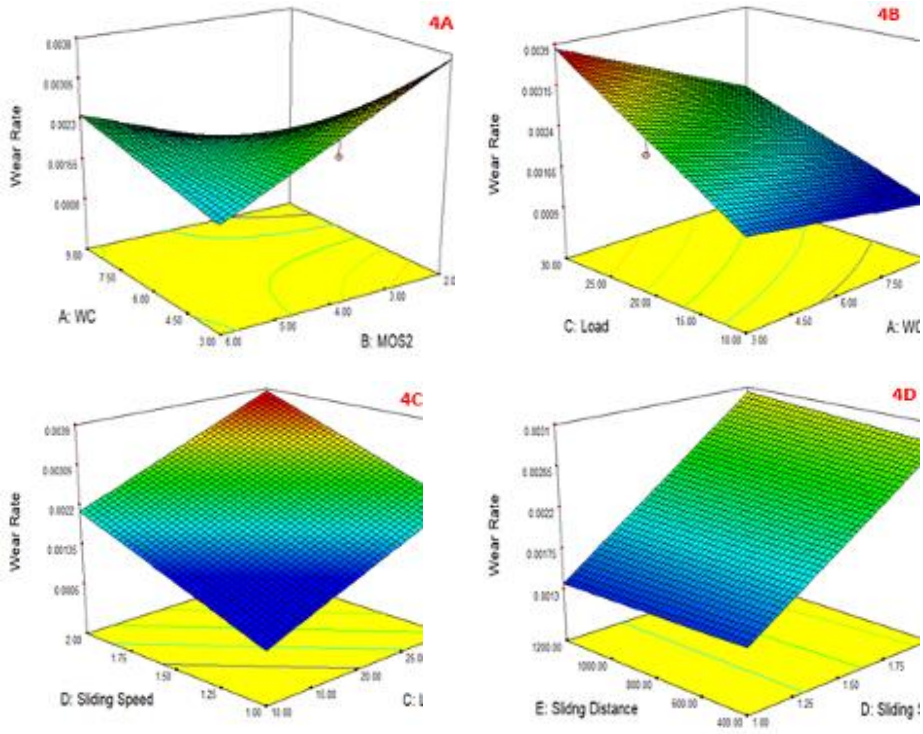

Fig. 4. Contour plot for input parameters Vs wear rate

The COF is shown in the graph is decreases up to 1 m/s before starting to rise as sliding speed increases rapidly [24]. The continuous development of a tribo layer at the contact surface is increased as sliding speed increases. Despite the fact that temperature increase increases as sliding velocity rises, the heat is in some ways beneficial for the development of a WC enrich interfacial layer, which in turn influences the development of compact layers at the contact area. However, when the sliding speed is increased beyond 1.5 m/s, a considerable quantity of heat is produced, which leads to the development of the composite pin softness results in increased in friction.

The figure 4A shows the contour plot for tungsten carbide and MoS_2 on wear rate. The graph indicates when the percentage of tungsten carbide increases from 3% to 6%. Wear rate is reduced from 0.0035 to 0.00275. When the weight percentage of tungsten carbide is 9 % the wear rate is less than 0.0015 grams this is mainly due to the density of the composite is higher so the loss of carbide particles which trends decrease in wear rate Also when the percentage of MoS2 at 6% offers minimum wear rate due to its self-lubrication properties of MoS_2[25]. The figure 4B shows the interaction graph of applied load and percentage of tungsten carbide on wear rate. Both the matrix alloys and the composites showed a direct relationship between weight loss and applied load. When the load is increased from 20N to 30 N the wear rate of material is high. However, when the weight percentage of reinforcement increases, the wear rate somewhat decreased. Both weight loss during the same applied load increased approximately continuously as sliding distance increased [25]. Figure 4C and 4D shows the interaction graph of applied load and sliding speed and sliding distance on wear rate. Additionally, it was found that as the

applied load increased up to its maximum, the effect of the sliding distance grew more severe. This might be connected to the heat created when the two abrasive connecting portions were engaged in the process of abrasive wear [26]. The test material softened as a result of the produced heat, which increased as the sliding distance.

The figure 5A shows the contour plot for tungsten carbide and MoS_2 on coefficient of friction. The friction between the pin and the disc is low when the weight Percentage of WC is increased. Initially the contact if friction at 3 % to 6% the friction between the plates is slightly decreased. Further when the percentage of WC is at 9% and at 6 % of MoS_2 the friction between the pin and disc is reduced. The figure 5B shows the interaction plot for wt. % of tungsten carbide and applied load on coefficient of friction. The impact of applied load on the resistance to wear reduced as the weight percentage of reinforcing particles increases. This may be explained by the addition of tungsten carbide particles mixed the matrix alloy, which increased hardness and decreased real area of contact, hence enhancing reducing of friction coefficient [27]. It is clear that the reinforcing particles can function as load-bearing components in composite made of aluminum composites, improving their friction. The figure 5C and figure 5D shows the interaction plot for sliding speed, Sliding distances and applied load on coefficient of friction. When the sliding velocity is increased from 1.5 m/sec to 2 m/sec the fiction between the pin and disc increases. The largest abrasion occurs at higher applied loads and highest sliding distances, producing excess heat in the two contacting surfaces and softening the interracial interactions between the matrix and reinforcement [28]. However, the effect of the applied load became more essential as the sliding distance increased.

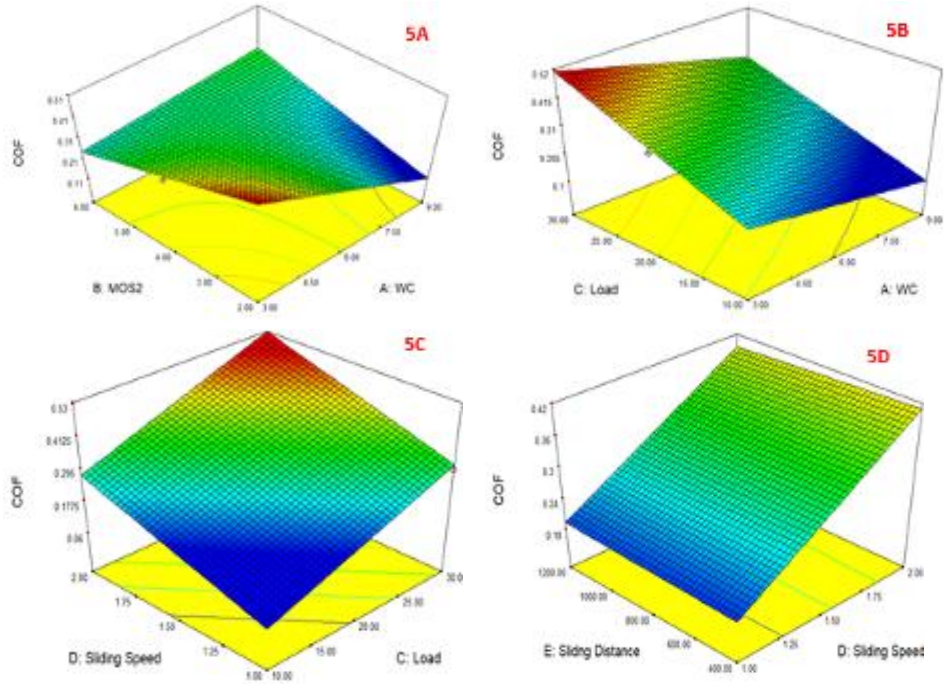

Fig. 5. Contour plot for input parameters vs coefficient of friction

Table 5. ANOVA for Wear Rate

Source	Sum of Square	df	Mean Square	F	p-value
Model	1.23E-05	9	1.37E-06	9.72	0.0001
A-WC	2.21E-06	1	2.21E-06	15.7	0.001
B-MoS2	8.25E-08	1	8.25E-08	0.59	0.0043
C-Load	3.93E-06	1	3.93E-06	27.95	0.0001
D-Sliding Speed	1.60E-06	1	1.60E-06	11.34	0.0037
E-Sliding Distance	1.08E-08	1	1.08E-08	0.076	0.0078
AB	1.35E-06	1	1.35E-06	9.59	0.0066
AC	9.65E-08	1	9.65E-08	0.69	0.0193
BC	2.26E-07	1	2.26E-07	1.6	0.0227
DE	2.90E-08	1	2.90E-08	0.21	0.0556
Residual	2.39E-06	17	1.41E-07		
Cor Total	1.47E-05	26			
R Square	91.20%				

ANOVA (Analysis of Variance) can be employed as a statistical method to analyze and compare the means of wear rates and coefficients of friction among multiple groups or experimental conditions. The ANOVA is employed for weight fraction of WC, MoS_2, applied load, sliding speed and sliding distance. Table 5 and 6 shows the ANOVA value for wear rate and coefficient of friction. The results shows that weight percentage of WC and applied load are the most significant parameters which influences wear rate and coefficient of friction.

Table 6. ANOVA for coefficient of friction

Source	Sum of Square	df	Mean Square	F	p-value
Model	0.25	10	0.025	13.59	0.0001
A-WC	0.049	1	0.049	26.39	0.0001
B-MOS2	5.14E-04	1	5.14E-04	0.28	0.0605
C-Load	0.081	1	0.081	43.59	0.0001
D-Sliding Speed	0.03	1	0.03	16.03	0.001
E-Sliding Distance	5.56E-06	1	5.56E-06	3.01E-03	0.0957
AB	0.024	1	0.024	12.78	0.0025
AC	2.60E-04	1	2.60E-04	0.14	0.0712
BC	2.01E-03	1	2.01E-03	1.09	0.0312
CE	3.00E-06	1	3.00E-06	1.62E-03	0.0684
DE	4.81E-04	1	4.81E-04	0.26	0.0168
Residual	0.03	16	1.85E-03		
Cor Total	0.28	26			
R Square	92.29				

4.2 Regression Equation

Regression equations are mathematical models that help in understanding and predicting the relationship between two or more variables. The equation 3 and 4 shows the mathematical model for wear rate and coefficient of friction.

$$\text{Wear Rate} = +2.175E\text{-}003 - 5.297E\text{-}004 * A - 1.279E\text{-}004 * B + 8.835E\text{-}004 * C + 7.878E\text{-}004 * D + 2.444E\text{-}005 * E + 8.781E\text{-}004 * A * B - 2.348E\text{-}004 * A * C - 2.538E\text{-}004 * B * C + 4.917E\text{-}005 * D * E \quad (3)$$

$$COF = +0.30 - 0.079 * A - 0.010 * B + 0.1 * C + 0.11 * D - 5.556E\text{-}004 * E + 0.12 * A * B - 0.012 * A * C - 0.024 * B * C + 5.000E\text{-}004 * C * E - 6.333E\text{-}003 * D * E \quad (4)$$

4.3 Microstructure Analysis

The Figure 6a shows the worn-out surface which is identified through SEM images. Figure 6 a show the 9 % of WC and 4 % of MoS_2 and load of 10N. The figure 6b shows that 9 % of WC and 6 % of MoS_2 and load of 10N. When compared to figure 6a figure 6b has reduction in wear rate. Also, it can be found that the WC particles also have less worn-out area owing to its hardness value. It is commonly accepted that adding hard particles to aluminum alloys enhances the underlying alloy's wear resistance to a noticeable extent [29]. Good surface adhesion occurs between the matrices and non-reinforcement whenever refractory bits are firmly bonded to the matrix. According to numerous studies, the COF of crystalline MoS_2 is typically low, at 6% in a dry sliding condition, this lubricating performance of MoS_2 is unique due to its self-lubrication properties. Figure 6 c shows the 6 % of WC and 6 % of MoS_2 and load of 20N. The figure 6c shows that 6 % of WC and 4 % of MoS_2 and load of 20N. When compared to figure 6d figure 6c exhibits better wear resistance. This is due to increased surface temperatures at the contact area encouraged the formation of low shear strength thermo on the rubbing surfaces [30]. The reduced resistive values were caused by a protecting tribo layer that accumulated on the surface of the materials at slower sliding speeds [31].

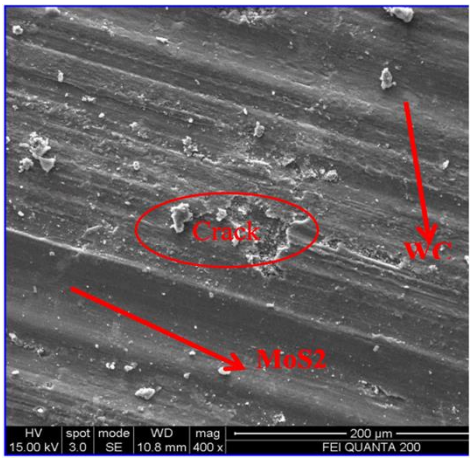

Fig. 6a. 9% WC & 4% MoS2, Load 10N

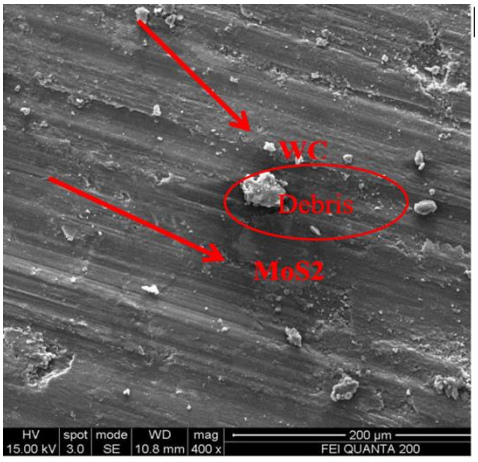

Fig. 6b. 9 % WC & 6 % of MoS_2, Load 10N

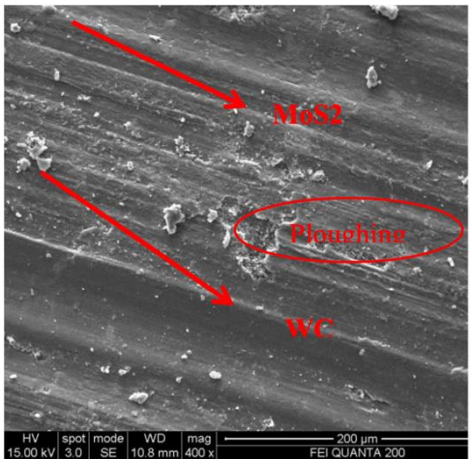

Fig. 6c. 6% WC & 6% of MoS_2, Load 20N

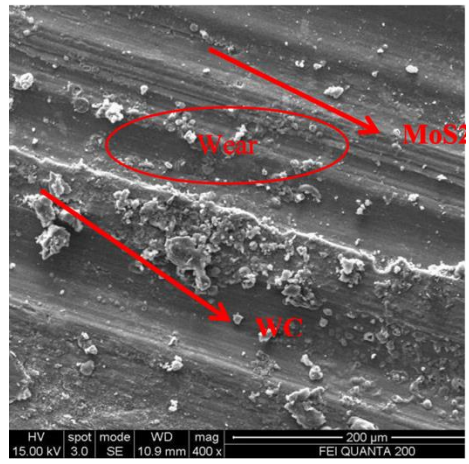

Fig. 6d. 6% of WC & 4% of MoS_2, Load 20N

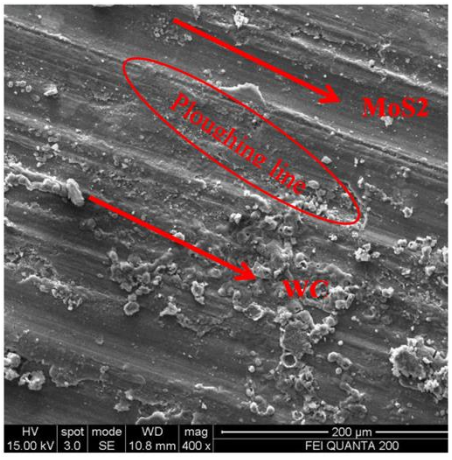

Fig 6e: 3% WC & 4% MoS_2, Load 30N

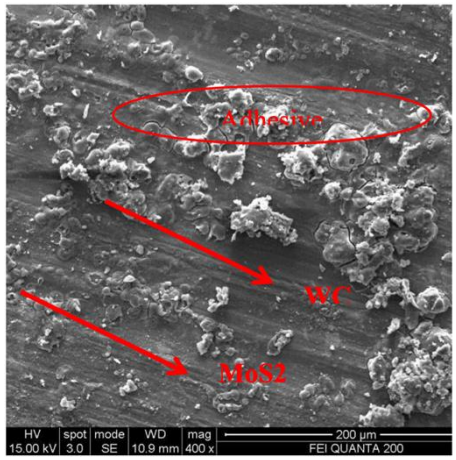

Fig. 6f. 3% WC & 2% MoS_2, Load 30N

For a fixed sliding velocity, the rapid tribo layer covering formation at higher speeds tends to reduce the surface hardness of the composites. Figure 6e shows the 3 % of WC and 4 % of MoS_2 and load of 30N. The figure 6f shows that 3 % of WC and 2 % of MoS_2 and load of 30N. When compared to figure 6e figure 6f has significant loss of tungsten carbide particles due to low addition of MoS_2 particles. When the load reaches 30 N, the wear rate dramatically increases. In the event that the Composite's changeover load and velocity both significantly rise in higher load value. The rationalized adhesion of the pin substance to the counter surface, the increase in the softening of the surface structure, and the ability of more abrasive particles to penetrate the surface of the composites [32].

5. Conclusion

In this recent experiment, we successfully fabricated Al 6262/WC/MoS_2 hybrid composites using the stir casting technique, incorporating various weight percentages of Tungsten Carbide (WC) – specifically, 3%, 6%, and 9%. Taguchi optimization was applied to determine the optimal combination of input parameters for achieving improved wear rates and friction reduction. The experiment yielded important conclusions:

At a composition of 9% WC and 4% MoS_2, the hardness reached 92.2 BHN. An increase in the weight percentages of both tungsten carbide and MoS2 was found to enhance hardness, consequently leading to a reduction in wear rates. Taguchi optimization highlighted that the optimum combination for minimizing wear rates involved 9% WC, 6% MoS_2, a 10N load, a sliding velocity of 1 m/sec, and a sliding distance of 400 m. The incorporation of hard particles significantly improved the wear resistance of the aluminum alloy base.

For achieving the lowest coefficient of friction, the optimal combination was identified as 9% WC, 6% MoS_2, a 10N load, a sliding velocity of 1 m/sec, and a sliding distance of 400 m. Successful surface adhesion occurred between the matrices and non-reinforcement, particularly when refractory bits firmly bonded to the matrix. The addition of tungsten carbide particles to the matrix alloy increased hardness and reduced the real area of contact, thereby enhancing the reduction of the friction coefficient.

SEM analysis validated worn-out surfaces during dry sliding wear. The maximum occurrences of grooving, ploughing, micro-cutting, fracturing, and embrittlement were observed in the composite with 3% WC and 2% MoS_2 under a 30N load. This phenomenon was attributed to increased surface temperatures at the contact area, promoting the formation of a low shear strength thermo-affected layer on the rubbing surfaces. The reduced resistive values were linked to the presence of a protective tribo layer accumulating on the material surface, particularly under increased loads, resulting in a severe wear rate.

References

[1] Borenstein A, Hanna O, Attias R, Luski S, Brousse T, Aurbach D. Carbon-based composite materials for supercapacitor electrodes: a review. Journal of Materials Chemistry A, 2017; 5(25):12653-12672. https://doi.org/10.1039/C7TA00863E

[2] Zhang Z, Xiao F, Qian L, Xiao J, Wang S, Liu Y. Facile synthesis of 3D MnO2-graphene and carbon nanotube-graphene composite networks for high-performance, flexible, all-solid-state asymmetric super capacitors. Advanced Energy Materials, 2014; 4(10): 1400064. https://doi.org/10.1002/aenm.201400064

[3] Roy Atanu, Apurba Ray, Samik Saha, Monalisa Ghosh, Trisha Das, Biswarup Satpati, Mahasweta Nandi, Sachindranath Das. NiO-CNT composite for high performance supercapacitor electrode and oxygen evolution reaction. Electrochimica Acta, 2018; 283: 327-337. https://doi.org/10.1016/j.electacta.2018.06.154

[4] Sahu SR, Rikka VR, Haridoss P, Chatterjee A, Gopalan R, Prakash R. A novel α-MoO3/single-walled carbon nanohorns composite as high-performance anode material for fast-charging lithium-ion battery. Advanced Energy Materials, 2020;10(36): 2001627. https://doi.org/10.1002/aenm.202001627

[5] Lou Zheng, Lili Wang, Kai Jiang, Zhongming Wei, Guozhen Shen. Reviews of wearable healthcare systems: Materials, devices and system integration. Materials Science and Engineering Reports, 2020; 140: 100523. https://doi.org/10.1016/j.mser.2019.100523

[6] Anil Kumar R, Radhika N. Enhancement of mechanical and wear properties of tungsten carbide coated AA 6063 alloy using detonation gun technique. Transactions of the IMF, 2018; 96 (4):212-219. https://doi.org/10.1080/00202967.2018.1477265

[7] Balaraj V, Nagaraj Kori, Madeva Nagaral, Auradi V. Microstructural evolution and mechanical characterization of micro Al2O3 particles reinforced Al6061 alloy metal composites. Materials Today: Proceedings, 2021; 47: 5959-5965. https://doi.org/10.1016/j.matpr.2021.04.500

[8] Raksha MS, Madeva Nagaral, Satish Babu Boppana, Chandrashekar Anjinappa, Mohammad Shahiq Khan, Mohammed Osman Abdul Wahab, Saiful Islam, Vivek Bhardwaj, Rohini Kumar Palavalasa, Mohammad Amir Khan, Abdul Razak, Impact of

boron carbide particles and weight percentage on the mechanical and wear characterization of Al2011 alloy metal composites, ACS Omega, 2023; 8, 26:23763-23771. https://doi.org/10.1021/acsomega.3c02065

[9] Madeva N, Shivananda BK, Virupaxi A, Kori SA. Development and mechanical-wear characterization of Al2024-nano B4C composites for aerospace applications. Strength, Fracture and Complexity, 2020; 13, 1:1-13. https://doi.org/10.3233/SFC-190248

[10] Gupta JG, Avinash KA. Engine durability and lubricating oil tribology study of a biodiesel fuelled common rail direct injection medium-duty transportation diesel engine. Wear, 2021; 486: 204104. https://doi.org/10.1016/j.wear.2021.204104

[11] Manivannan I, Ranganathan S, Gopalakannan S, Suresh S. Mechanical properties and tribological behavior of Al6061-SiC-Gr self-lubricating hybrid nanocomposites. Transactions of the Indian Institute of Metals, 2018; 71, 8: 1897-1911. https://doi.org/10.1007/s12666-018-1321-0

[12] Saravanakumar A, Bhuvaneswari V, Karthick Raja N, Karthi P. Tribological behaviour of AA2219/MoS2 metal matrix composites under lubrication. AIP Conference Proceedings, 2020; 2207.

[13] Jojith, Radhika N. Mechanical and tribological properties of LM13/TiO2/MoS2 hybrid metal matrix composite synthesized by stir casting. Particulate Science and Technology, 2019; 37 (5): 570-582. https://doi.org/10.1080/02726351.2017.1407381

[14] Madeva Nagaral, Auradi V, Bharath V. Mechanical characterization of 100 micron sized silicon carbide particles reinforced Al6061 alloy composites. Metallurgical and Materials Engineering, 2022; 28 (1): 17-32. https://doi.org/10.30544/639

[15] Siddeshkumar NG, Suresh R, and Shiva Shankar GS. High temperature wear behavior of Al2219/n-B4C/MoS2 hybrid metal matrix composites. Composites Communications, 2020; 19: 61-73. https://doi.org/10.1016/j.coco.2020.02.011

[16] Preethi K, Raju TN, Shivappa HA, Shashidhar S, Madeva Nagral. Processing, microstructure, hardness and wear behavior of carbon nanotube particulates reinforced Al6061 alloy composites. Materials Today: Proceedings, 2023; 81: 449-453. https://doi.org/10.1016/j.matpr.2021.03.608

[17] Kumar C, Ramesh R, Malarvannan, Jaiganesh V. Role of SiC on mechanical, tribological and thermal expansion characteristics of B4C/Talc-reinforced Al-6061 hybrid composite. Silicon, 2020; 12 (6): 1491-1500. https://doi.org/10.1007/s12633-019-00243-0

[18] Pankaj J, Sridhar , Madeva N, Vijay KM, Jayasheel H. A comparative study on microstructure and mechanical properties of A356-B4C and A356-Graphite composite. International Journal of Mechanical and Production Engineering Research and Development, 2018; 8 (2): 273-282. https://doi.org/10.24247/ijmperdapr201830

[19] Zhai W, L B, Runhua Z, Xueling F, Guozheng K, Yong L, Kun Z. Recent progress on wear-resistant materials: designs, properties, and applications. Advanced Science, 2021; 8 (11): 2003739. https://doi.org/10.1002/advs.202003739

[20] Moazami G, Mohammad, A Ne. Tribological behavior of self lubricating Cu/MoS2 composites fabricated by powder metallurgy. Transactions of Nonferrous Metals Society of China, 2018; 28 (5): 946-956. https://doi.org/10.1016/S1003-6326(18)64729-6

[21] Kumar , Saravanan R, Madeva Nagaral. Dry sliding wear behavior of nano boron carbide particulates reinforced Al2214 alloy composites. Materials Today: Proceedings, 2023; 81: 191-195. https://doi.org/10.1016/j.matpr.2021.03.065

[22] Alaneme KK, Adetomilola V F, Nthabiseng B M. Development of aluminium-based composites reinforced with steel and graphite particles: structural, mechanical and wear characterization. Journal of Materials Research and Technology, 2019; 8(1): 670-682. https://doi.org/10.1016/j.jmrt.2018.04.019

[23] Zhang Y, Panpan L, Li Ji Xiaohong L, Hongqi W, Lei Ch, Hongxuan L Zhiliang J. Tribological properties of MoS2 coating for ultra-long wear-life and low coefficient of friction combined with additive g-C3N4 in air. Friction, 2021; 9(4): 789-801. https://doi.org/10.1007/s40544-020-0374-3

[24] Öztürk B, Fazlı A, Sultan Ö. Hot wear properties of ceramic and basalt fiber reinforced hybrid friction materials. Tribology International, 2007; 40(1): 37-48. https://doi.org/10.1016/j.triboint.2006.01.027

[25] Saravanakumar ABhuvaneswari V, Gokul G. Optimization of wear behaviour for AA2219-MoS2 metal matrix composites in dry and lubricated condition. Materials Today: Proceedings, 2020; 27: 2645-2649. https://doi.org/10.1016/j.matpr.2019.11.087

[26] Bharathi V, Ramachandra M, Srinivas S. Influence of fly ash content in aluminium matrix composite produced by stir-squeeze casting on the scratching abrasion resistance, hardness and density levels. Materials Today: Proceedings, 2017;4(8): 7397-7405. https://doi.org/10.1016/j.matpr.2017.07.070

[27] Nemati N, Khosroshahi R, Emamy M, Zolriasatein A. Investigation of microstructure, hardness and wear properties of Al-4.5 wt.% Cu-TiC nanocomposites produced by mechanical milling. Materials and Design, 2011; 32 (7): 3718-3729. https://doi.org/10.1016/j.matdes.2011.03.056

[28] Jalilvand MM, Yousef MEffect of mono and hybrid ceramic reinforcement particles on the tribological behavior of the AZ31 matrix surface composites developed by friction stir processing. Ceramics International, 2020; 46(12): 20345-20356. https://doi.org/10.1016/j.ceramint.2020.05.123

[29] Murali MR, Kempaiah UN, Manjunatha B, Madeva N, Auradi V. Processing and wear behavior optimization of B4C and rice husk ash dual particles reinforced ADC12 alloy composites using Taguchi method. Materials Physics & Mechanics, 2022; 50, 2:304-318.

[30] Madeva Na, Deshapande RG, Auradi V, Satish BB, Samuel D, Anilkumar MR. Mechanical and wear characterization of ceramic boron carbide reinforced Al2024 alloy metal composites. Journal of Bio-and Tribo-Corrosion, 2021; 7: 1-12. https://doi.org/10.1007/s40735-020-00454-8

[31] Cimenoglu H, Atar E, Motallebzadeh A. High temperature tribological behaviour of borided surfaces based on the phase structure of the boride layer. Wear, 2014; 309(1-2): 152-158. https://doi.org/10.1016/j.wear.2013.10.012

[32] Daniel AA, Sakthivel M, Sudhagar S. Dry sliding wear behaviour of aluminium 5059/SiC/MoS2 hybrid metal matrix composites. Materials Research, 2017; 20: 1697-1706. https://doi.org/10.1590/1980-5373-mr-2017-0009